and J_{AB} = 14 Hz. If in the paramagnetic Co(OEPR$_2$) there is not complete collapse of the ABX_3 multiplet structure, then the lines will be broader than calculated from eq 5 and possibly equal in line width throughout the series **1-4**. Thus it is debatable as to what effect, if any, "hindered rotation" of α-CH_2 has upon the NMR spectra of these porphodimethenes.

Similar steric crowding of the α-CH_2 groups has also been proposed for OEP complexes. La Mar and Walker alluded to the "severely restricted rotation" of the α-CH_2 groups in [Fe(OEP)(Im)$_2$]Cl because a plot of $(\Delta H/H)_{iso}$ was linear with T for these protons.[41] However, other compounds, for example Fe(OEP)[42] and [Fe(OEP)(pip)$_2$]Cl,[43] exhibit linear $(\Delta H/H)_{iso}$ vs. T^{-1} plots for α-CH_2. Thus there is also ambiguity for OEP complexes.

Base Addition to Co(OEPR$_2$). Because the dialkylporphodimethenes have an intrinsic asymmetry, one can in principle determine whether axial coordination of base occurs from the top (syn-axial) or bottom (anti-axial). This will be illustrated for the addition of 1-methylimidazole (1-MeIm) to Co(OEPBu$_2$). When small amounts of 1-MeIm in toluene-d_8 are added to Co(OEPBu$_2$), the porphodimethene proton resonances broaden quickly and coalesce toward the diamagnetic region. Axial ligand exchange is rapid on the NMR time scale, and the resonance positions are a mole fraction average of that in Co(OEPBu$_2$) and Co(OEPBu$_2$)·1-MeIm. The diminished isotropic shifts in the five-coordinate species have been attributed to a smaller magnetic anisotropy in square-pyramidal cobalt(II); the line broadening has been explained by a decrease in T_{1e} upon axial addition.[19]

If one assumes that upon axial addition no major structural changes occur other than the metal moving out of the tetraaza plane toward the 1-MeIm, then one can compare relative proton line widths of Co(OEPBu$_2$) as a function of added ligand and obtain useful structural information. As an example, the line widths of 5-H and 10-H in Co(OEPBu$_2$) were monitored as a function of added 1-MeIm. In all porphodimethenes 5-H sits above the tetraaza plane (+Z coordinate) whereas 10-H is located below the tetraaza plane (-Z coordinate). For Co(OEPBu$_2$) axial coordination can occur only from the bottom since the top side is blocked effectively by the bulky syn-axial *tert*-butyl groups. Upon coordination of base, the cobalt atom will move downward, closer to 10-H but more distant from 5-H. Thus one expects $(\Delta\nu_{1/2})_{5\text{-H}}/(\Delta\nu_{1/2})_{10\text{-H}}$ to decrease as a function of added base. Were axial coordination to occur from the top side, the aforementioned ratio would increase instead.

Experimentally when 1-MeIm in toluene-d_8 was added in small increments to a solution of Co(OEPBu$_2$) in toluene-d_8, the aforementioned line width ratio *decreased* as expected from a initial value of 1.28 to 1.09, at which point the lines became too broad for precise measurement. This suggests axial coordination from the bottom, unhindered side. For 100% adduct formation with cobalt displaced 0.10 Å below the tetraaza plane, as in Co(OEPBu$_2$)NO, our geometrical model predicts $(\Delta\nu_{1/2})_{5\text{-H}}/(\Delta\nu_{1/2})_{10\text{-H}}$ = 0.851. Addition of 1-MeIm to Co(OEPMe$_2$) yielded equivocal results with no discernable trend in $(\Delta\nu_{1/2})_{5\text{-H}}/(\Delta\nu_{1/2})_{10\text{-H}}$. Since Co(OEPMe$_2$) can coordinate from either top or bottom, both processes may occur concurrently with near-equal probability.

Acknowledgment. We are grateful to the Deutsche Forschungsgemeinschaft for its generous support of this work, to the Vereinigung der Freunde der Technischen Hochschule, Darmstadt, West Germany, and to NATO for a collaborative research grant. We also thank Drs. S. Braun, G. Cordier, and K. Wannowius for their invaluable assistance.

Registry No. **1**, 97805-52-2; **2**, 97732-92-8; **3**, 97732-93-9; **4**, 97805-53-3; $Co_2(CO)_8$, 10210-68-1.

(41) La Mar, G. N.; Walker, F. A. *J. Am. Chem. Soc.* **1973**, *95*, 1782
(42) Mispelter, J.; Momenteau, M.; Lhoste, J. M. *Mol. Phys.* **1977**, *33*, 1715.
(43) Morishima, I.; Kitigawa, S.; Matsuki, E.; Inubushi, T. *J. Am. Chem. Soc.* **1980**, *102*, 2429.

Contribution from the Department of Chemistry, Purdue University, West Lafayette, Indiana 47907

Characterization of Bis(tripeptido)nickelate(III) Complexes in Aqueous Solution

GEORGE E. KIRVAN and DALE W. MARGERUM*

Received January 24, 1985

Addition of excess tripeptide (L^-) to solutions of (tripeptido)nickel(III), $Ni^{III}(H_{-2}L)$, gives bis(tripeptido)nickelate(III) complexes. In the initial reaction $[Ni^{III}(H_{-2}L)L]^-$ forms, but it is a transitory species that rapidly loses a proton to give $[Ni^{III}(H_{-2}L)(H_{-1}L)]^{2-}$, a complex with five nitrogens coordinated to nickel. This five-nitrogen complex is relatively stable from pH 6 to 11. It converts to a six-nitrogen tetragonally elongated complex, $[Ni^{III}(H_{-2}L)_2]^{3-}$, above pH 11. The bis complexes of G_3^- are 10^3-10^6 times slower to undergo base-catalyzed redox decomposition than are the corresponding mono complexes of nickel(III). The bis(glycyl-L-alanylglycinato) complex, $[Ni^{III}(H_2GAG)(H_1GAG)]^{2-}$, dissociates in acid to form $Ni^{III}(H_{-2}GAG)$ with a first-order rate constant of 34 s^{-1} (25.0 °C) from pH 1.5 to 3.5. Electron-transfer reactions of the bis complexes occur via outer-sphere mechanisms, and the bis(tripeptido)nickelate(II) complex produced dissociates rapidly to $Ni^{II}(H_{-2}L)^-$. The reduction potentials of the bis complexes are estimated to be less than 0.24 V (vs. NHE).

Introduction

Deprotonated oligopeptide complexes of nickel(III) have been shown to be moderately stable in aqueous media.[1,2] Electron paramagnetic resonance studies[3-5] indicate that nickel(III)-tripeptide complexes have tetragonally elongated geometry with water molecules in the axial sites (z axis)[6] and with the unpaired electron in the d_{z^2} oribtal. The nature of the tripeptide ligand has relatively little effect on the reduction potential of the mono complexes. Values of $E^{\circ\prime}$ vary from 0.80 to 0.89 V (vs. NHE) for different tripeptide complexes.[2]

Recently, nickel(III) has been found in several nickel-containing bacteria.[7-11] Hydrogenase from *Desulfovibrio gigas* reportedly contains one nickel(III) per enzyme molecule and has a reduction

(1) Bossu, F. P.; Margerum, D. W. *J. Am. Chem. Soc.* **1976**, *98*, 4003-4004.
(2) Bossu, F. P.; Margerum, D. W. *Inorg. Chem.* **1977**, *16*, 1210-1214.
(3) Lappin, A. G.; Murray, C. K.; Margerum, D. W. *Inorg. Chem.* **1978**, *17*, 1630-1634.
(4) Sugiura, Y.; Mino, Y. *Inorg. Chem.* **1979**, *18*, 1336-1339.
(5) Sakurai, T.; Hongo, J.; Nakahara, A.; Nakao, Y. *Inorg. Chim. Acta* **1980**, *46*, 205-210.
(6) Youngblood, M. P.; Margerum, D. W. *Inorg. Chem.* **1980**, *19*, 3068-3072.
(7) Cammack, R.; Patil, D.; Aguirre, R.; Hatchikian, E. C. *FEBS Lett.* **1982**, *142*, 289-292.
(8) Thomson, A. J. *Nature (London)* **1982**, *298*, 602-603.
(9) Ragsdale, S. W.; Ljungdahl, L. G.; DerVartanian, D. V. *Biochem. Biophys. Res. Commun.* **1982**, *108*, 658-663.
(10) Albracht, S. P. J.; Graf, E. G.; Thauer, R. K. *FEBS Lett.* **1982**, *140*, 311-313.
(11) Kojima, N.; Fox, J. A.; Hausinger, R. P.; Daniels, L.; Orme-Johnson, W. H.; Walsh, C. *Proc. Natl. Acad. Sci. U.S.A.* **1983**, *80*, 378-382.

0020-1669/85/1324-3245$01.50/0

potential of −0.145 V.[7] The coordination environment of the biological nickel(III) is not well characterized, and the reason for the very low reduction potential is not clear. We are interested in determination of some of the factors that lower the reduction potential of Ni(III/II) couples and stabilize the trivalent oxidation state. This is the case with the bis(tripeptide) complexes, although we do not suggest that they are necessarily models for biological nickel.

Bis(peptide) complexes of nickel(III) were proposed in earlier studies[3,12] and appeared to be more stable to redox decomposition than mono(peptide) complexes of nickel(III). Recently, the solution properties of bis(dipeptido)nickelate(III) complexes were investigated.[13] The latter complexes have both tetragonally compressed and tetragonally elongated geometries, and their reduction potentials are estimated to be in the range 0.66–0.83 V (vs. NHE).

In the present study, EPR and other evidence are used to propose structures for two different bis(tripeptide) complexes of nickel(III). These complexes are 10^3–10^6 times slower to undergo base-catalyzed redox decomposition than the mono complexes. Their estimated reduction potentials are less than 0.24 V (vs. NHE). The kinetics and proposed mechanisms of formation, acid dissociation, base-catalyzed decomposition, and electron-transfer reactions are reported.

Experimental Section

Nickel(II) perchlorate was prepared from $NiCO_3$ and $HClO_4$. After recrystallization, solutions were prepared and standardized by EDTA titration with murexide indicator. Di-α-aminoisobutyryl-α-aminoisobutyric acid (Aib_3) and its amide (Aib_3a) were synthesized by Hamburg.[14,15] Other peptides (chromatographically pure) were obtained from Biosynthetika or Vega-Fox. Abbreviations for other amino acid residues are as follows: G, glycyl; A, L-alanyl; F, L-phenylalanyl; leu, L-leucyl.

(Tripeptido)nickelate(II) complexes were prepared by slow addition of NaOH to solutions containing $Ni(ClO_4)_2$ and 10–400% excess tripeptide.[16] Each solution was raised to pH 10.0 in order to ensure complete formation of the doubly deprotonated complexes.

Solutions of (tripeptido)nickel(III) were prepared by electrochemical oxidation.[17,18] of the corresponding nickel(II) complexes in media containing 10% excess tripeptide. The nickel(III) solutions produced were adjusted to pH 5 with dilute $HClO_4$ in order to minimize redox decomposition. Bis(tripeptido)nickelate(III) solutions were made by two different methods. In one, excess tripeptide (300%) was added to solutions of the mono Ni(III) complexes. The solutions were slowly raised to pH 9 in order to form $Ni^{III}(H_{-2}L)(H_{-1}L)^{2-}$ or to pH 13 to form $Ni^{III}(H_{-2}L)_2^{3-}$ (L^- = tripeptide and H_{-n} indicates n-deprotonated peptide nitrogens). Alternatively, solutions of (tripeptido)nickelate(II) that contained 400% excess tripeptide were electrochemically oxidized, and the pH of the resulting nickel(III) solutions was then adjusted. The ionic strength of all solutions was maintained by $NaClO_4$ made from Na_2CO_3 and $HClO_4$, recrystallized and standardized gravimetrically.

Electron paramagnetic resonance spectra of magnetically dilute frozen aqueous glasses (<2 × 10^{-3} M Ni(III), −150 °C)[3] and of room-temperature solutions were obtained on a Varian E-109 X-band spectrometer modulated at 100 kHz. A Varian E-238 variable-temperature cavity and Varian E-238 variable-temperature controller were used for frozen samples. The multipurpose Varian E-231 cavity was used for room-temperature samples with a Wilmad WG-812 aqueous EPR cell. The magnetic field was calibrated relative to α,α′-diphenyl-β-picrylhydrazyl (DPPH), g = 2.004. A computer-generated spectral matching procedure was used to obtain g values and hyperfine coupling constants (A values).[3,13]

EPR also was used as a detector in a pH titration to determine the pK_a of one of the bis(tripeptido)nickelate(III) complexes. A peristaltic pump circulated solution from the titration vessel into the aqueous EPR cell and back to the titration vessel. Use of this flow system eliminated the need to remove the cell from the EPR cavity in order to change the pH of the sample. Slight changes in the position of the cell in the cavity may give rise to large errors in the determination of sample concentration.

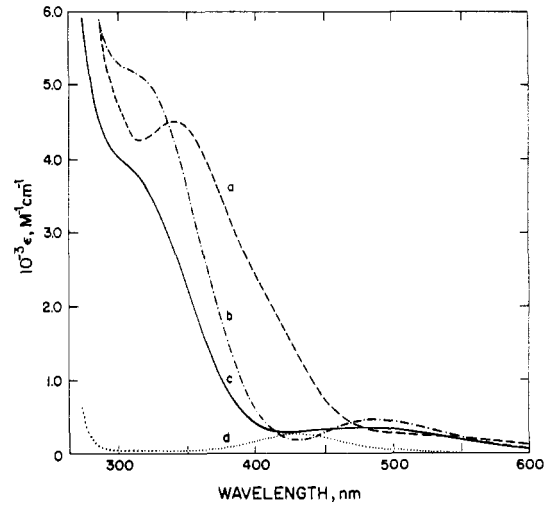

Figure 1. UV–visible spectra of nickel triglycine complexes: (a) 1.0 × 10^{-3} M $Ni^{III}(H_{-2}G_3)$; (b) $Ni^{III}(H_{-2}G_3)(H_{-1}G_3)^{2-}$ formed from 1.0 × 10^{-3} M $Ni^{III}(H_{-2}G_3)$ and 3.0 × 10^{-3} M G_3 at pH 9; (c) $Ni^{III}(H_{-2}G_3)_2^{3-}$ formed from 1.0 × 10^{-3} M $Ni^{III}(H_{-2}G_3)$ and 3.0 × 10^{-3} M G_3^- in 0.1 M NaOH; (d) 1.0 × 10^{-3} M $Ni^{II}(H_{-2}G_3)^-$.

Chromatographic determinations were performed on an IBM Instruments LC/9533 liquid chromatograph equipped with a LC/9523 variable-wavelength UV detector and a Hewlett-Packard 3390A integrator. An IBM Instruments 5-μm C_{18} column (25 × 0.45 cm) was used with 0.15 M phosphate buffer (pH 2.0) as the mobile phase. The detector was set at 206 nm.

Ultraviolet–visible spectra were recorded on a Perkin-Elmer 320 spectrophotometer equipped with a Perkin-Elmer 3600 data station. Kinetics were measured at 25.0 ± 0.1 °C on a Cary 16 or Durrum stopped-flow spectrophotometer.[19]

Between pH 2 and 11, hydrogen ion concentrations were measured with an Orion Research Model 601A pH meter equipped with a Corning 476051 combination electrode. The electrode was calibrated to give −log $[H^+]$ at various ionic strengths by means of perchloric acid–sodium hydroxide titrations.

Stability constants of several nickel(II) bis(peptide) and tris(peptide) complexes were determined by potentiometric titrations. The titrations were performed with an Orion Research Model 701A digital ionanalyzer equipped with a Sargent-Welch S30050-15C glass electrode and a saturated sodium chloride calomel reference electrode. Due to the high concentration of peptide needed to form the bis and tris complexes of nickel(II), the ionic strength was maintained at 1.0 M with $NaClO_4$. The reference electrode was connected to the titration vessel by an agar–agar salt bridge containing 1.0 M $NaClO_4$. The titrant, 1.0 M NaOH, was freshly prepared in order to minimize carbonate absorption, and H_2O-saturated argon was blown over the titration vessel also as a precaution against carbonate error. Solutions were thermostated at 25.0 ± 0.1 °C. Titrations were performed twice with solutions containing ligand only and with L:Ni ratios of 1:1 and 2:1. A $Ni(ClO_4)_2$ concentration of 5.0 × 10^{-2} M precluded higher L:Ni ratios because of the solubility limits of the ligand. The potentiometric data were analyzed by a modified version of the computer program SCOGS.[14] Cyclic voltammetry was performed with a three-electrode system consisting of a glassy-carbon, graphite, or carbon-paste working electrode, a platinum-wire auxiliary electrode, and a Ag/AgCl reference electrode. The working electrodes were preconditioned in the solvent by cycling between +1.5 and −1.5 V (vs. NHE).

Results and Discussions

Stoichiometry, Structure, and Equilibrium Constants. Electrochemical oxidation of a solution containing 1.0 × 10^{-3} M $Ni^{II}(H_{-2}G_3)^-$ and 3.0 × 10^{-3} M G_3^- or addition of 3.0 × 10^{-3} M G_3^- to a 1.0 × 10^{-3} M $Ni^{III}(H_{-2}G_3)$ solution yields a brown complex, which is stable for several hours in neutral or slightly alkaline solution. The UV–vis spectrum of the brown complex (Figure 1b) changes above pH 11 (Figure 1c). These complexes also have absorption shoulders at 242 and 240 nm, respectively,

(12) Bossu, F. P.; Paniago, E. B.; Margerum, D. W.; Kirksey, S. T., Jr.; Kurtz, J. L. *Inorg. Chem.* **1978**, *17*, 1034–1042.
(13) Jacobs, S. A.; Margerum, D. W. *Inorg. Chem.* **1984**, *23*, 1195–1201.
(14) Hamburg, A. W.; Nemeth, M. T.; Margerum, D. W. *Inorg. Chem.* **1983**, *22*, 3535–3541.
(15) Kirksey, S. T., Jr.; Neubecker, T. A.; Margerum, D. W. *J. Am. Chem. Soc.* **1979**, *101*, 1631–1633.
(16) Billo, E. J.; Margerum, D. W. *J. Am. Chem. Soc.* **1970**, *92*, 6811–6818.
(17) Murray, C. K.; Margerum, D. W. *Inorg. Chem.* **1983**, *22*, 463–469.
(18) Clark, B. R.; Evans, D. H. *J. Electroanal. Chem.* **1965**, *69*, 181–194.
(19) Willis, B. G.; Bittikofer, J. A.; Pardue, H. L.; Margerum, D. W. *Anal. Chem.* **1970**, *42*, 1340–1349.

Table I. Molar Absorptivities of G_3^- and G_2^- Complexes of Ni(III)[a]

complex	λ_{max}, nm	ϵ, M^{-1} cm^{-1}
$Ni^{III}(H_{-2}G_3)_2^{3-}$	240 sh	14019 (157)
	308 sh	4194 (49)
	466	475 (16)
$Ni^{III}(H_{-2}G_3)(H_{-1}G_3)^{2-}$	242 sh	14920 (114)
	320 sh	5126 (39)
	476	710 (16)
$Ni^{III}(H_{-2}G_3)$[b]	250	~11000
	340	4500 (150)
$Ni^{III}(H_{-1}G_2)_2^{-}$[c]	255	4800 (300)
	560	500 (30)

[a] ϵ values are given per Ni(III). [b] Reference 2. [c] Reference 13.

Scheme I

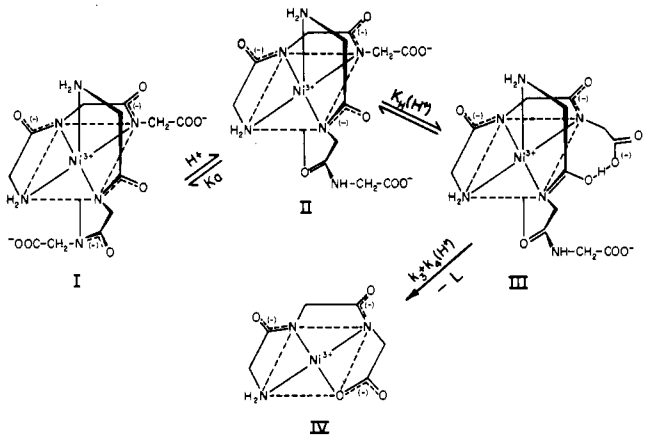

in agreement with typical absorption peaks found for other Ni(III) peptides.[2,13] The molar absorptivities of the two species, identified later as $Ni^{III}(H_{-2}G_3)(H_{-1}G_3)^{2-}$ and $Ni^{III}(H_{-2}G_3)_2^{3-}$, were determined by hexacyanoferrate(II) titration and are given in Table I.

Nickel(III)–peptide complexes have thus far been too unstable to obtain crystals for X-ray crystal structure determination. EPR studies frequently have been used to propose the structure of nickel(III) species.[3,13,20-22] Frozen-solution EPR spectra of the brown nickel(III) complexes at pH 9 and 13 are shown in Figure 2, along with the spectrum of $Ni^{III}(H_{-2}G_3)$ for comparison. The dashed line is the computer-simulated spectrum[23] using the g values and coupling constants obtained by spectral matching (Table II). In each case, the geometry of the complex is tetragonally elongated as indicated by the relative order of g values, $g_\perp > g_\parallel$.[3] Hyperfine splitting ($2I + 1$) seen in the high magnetic field portion of the spectra ($g_\parallel$ region) is indicative of the number of ^{14}N ($I = 1$) atoms coordinated axially.

The proposed formula of the brown complex at pH 9 is $Ni^{III}(H_{-2}G_3)(H_{-1}G_3)^{2-}$, structure II in Scheme I. Three peaks in the $g_\parallel$ region (Figure 2b) indicate one axial nitrogen is coordinated. The increased symmetry in the $g_\perp$ region compared to the $g_\perp$ region of $Ni^{III}(H_{-2}G_3)$ is reflected in the equal values for g_{xx} and g_{yy} (Table II), because the atoms in the equatorial plane are all nitrogens in II rather than three nitrogens and a carboxylate oxygen (IV). A water molecule, or a peptide oxygen as shown in II, may be coordinated at the second axial site. Indirect evidence presented in the electron-transfer section of this paper implies that a peptide oxygen is coordinated.

At pH 13, five peaks in the $g_\parallel$ region (Figure 2c) indicate that a second nitrogen is axially coordinated to nickel (structure I in Scheme I). The proposed formula is $Ni^{III}(H_{-2}G_3)_2^{3-}$, where there are six nitrogens, four of which are deprotonated *N*-peptide groups, coordinated to Ni(III). The deviation between the observed and calculated curves in Figure 2c is eliminated when the EPR spectrum is measured at −213 °C rather than at −150 °C. A dynamic Jahn–Teller distortion causes the EPR spectra of this species to be temperature dependent in the frozen state.[24]

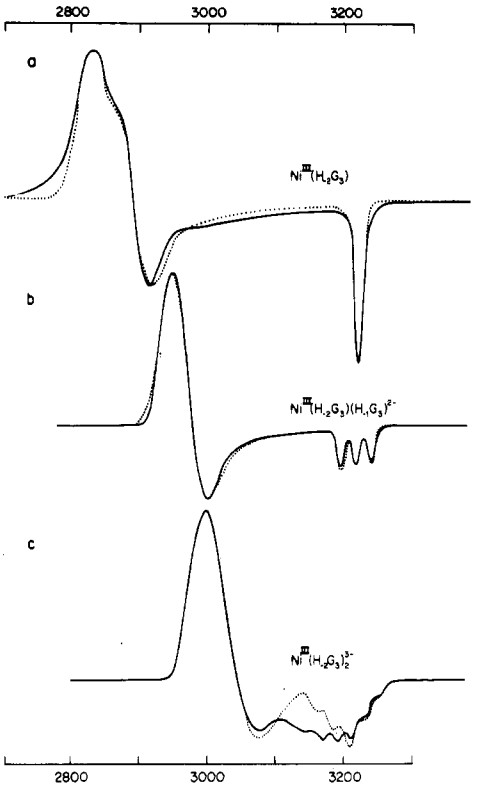

Figure 2. EPR spectra ((—), experimental; (···), calculated) for nickel(III) complexes of triglycine in magnetically dilute aqueous glasses at −150 °C; 9.079 GHz: (a) 1.0×10^{-3} M $Ni^{III}(H_{-2}G_3)$ at pH 5.0; (b) $Ni^{III}(H_{-2}G_3)(H_{-1}G_3)^{2-}$ formed from 1.0×10^{-3} M $Ni^{III}(H_{-2}G_3)$ and 3.0×10^{-3} M G_3 at pH 9.0; (c) $Ni^{III}(H_{-2}G_3)_2^{3-}$ formed from 1.0×10^{-3} M $Ni^{III}(H_{-2}G_3)$ and 3.0×10^{-3} M G_3 in 0.10 M NaOH.

The trend in g values of the triglycine complexes reported in Table II also supports these formulas. As the strength of axial coordination increases, the difference in energy between the d_{z^2} orbital and the d_{xz} and d_{yz} orbitals increases. Therefore, the g_{xx} and g_{yy} values decrease.[3] At the same time, vibronic mixing of the d_{z^2} and $d_{x^2-y^2}$ ground states increases and causes g_{zz} to increase slightly. This same trend has been shown previously for axial coordination of NH_3 and G_3a to nickel(III) complexes[3] (see Table II).

Formation of a tris complex, with two amine groups coordinated axially, would also show five peaks in the $g_\parallel$ region. However, this can be ruled out for two reasons. First, its formation would not be dependent on pH at pH 10–12 because this is well above the pK_a (7.88[16]) of the free triglycine. Second, the EPR and UV-vis spectra of 1.0×10^{-3} M nickel(III) solutions are independent of the triglycine concentration in the range 2.0×10^{-3} to 2.0×10^{-2} M.

The equilibrium constant for the overall formation reaction of $Ni^{III}(H_{-2}G_3)(H_{-1}G_3)^{2-}$, eq 1, was determined by UV–vis spectrophotometry (Table III) from a plot of the left side of eq 2 vs. $[G_3^-]/[H^+]$. The value of K_2 is $(3.2 \pm 0.2) \times 10^{-3}$ at $\mu = 0.1$.

$$Ni^{III}(H_{-2}G_3) + G_3^- \overset{K_2}{\rightleftharpoons} Ni^{III}(H_{-2}G_3)(H_{-1}G_3)^{2-} + H^+ \quad (1)$$

$$\frac{A - A_0}{A_\infty - A} = \frac{[G_3^-]}{[H^+]} K_2 \quad (2)$$

(20) Kirschenbaum, L. J.; Haines, R. I. *Inorg. Chim. Acta* **1983**, *76*, L127–L129.
(21) Lovecchio, F. V.; Gore, E. S.; Bush, D. H. *J. Am. Chem. Soc.* **1974**, *96*, 3109–3118.
(22) Haines, R. I.; McAuley, A. *Coord. Chem. Rev.* **1981**, *39*, 77–119.
(23) Toy, A. D.; Chaston, S. H. H.; Pilbrow, J. R.; Smith, T. D. *Inorg. Chem.* **1971**, *10*, 2219–2226.
(24) Pappenhagen, T. L.; Margerum, D. W., to be submitted for publication.

Table II. EPR Parameters of Nickel(III)–Peptide Complexes[a]

complex	g_{xx}	g_{yy}	g_{zz}	A_{zz}, G	W_{xx}	W_{yy}	W_{zz}	g_{av}[b]	g_{iso}[c]
$Ni^{III}(H_{-2}G_3)$	2.242	2.295	2.015		1.75	2.50	1	2.184	2.197
$Ni^{III}(H_{-2}G_3)(H_{-1}G_3)^{2-}$	2.198	2.198	2.016	20.0	3.84	3.84	1	2.137	2.142
$Ni^{III}(H_{-2}G_3)_2^{3-}$	2.151	2.151	2.021	19.5	2.00	2.00	1	2.108	2.115
$Ni^{III}(H_{-3}G_3a)$[d]	2.310	2.281	2.006		5.88	2.94	1	2.199	
$Ni^{III}(H_{-3}G_3a)(NH_3)$[d]	2.217	2.217	2.011	23.4	4.33	4.33	1	2.148	
$Ni^{III}(H_{-3}G_3a)(NH_3)_2$[d]	2.178	2.178	2.023	21.3	4.00	4.00	1	2.126	
$Ni^{III}(H_{-2}G_3a)(H_{-1}G_3a)$[d]	2.196	2.196	2.023	21.3	3.26	3.26	1	2.138	

[a] The spectra were obtained at $T = -150$ °C and are of aqueous glasses unless otherwise noted. $g_\perp = {}^1/_2(g_{xx} + g_{yy})$ and $g_\parallel = g_{zz}$. [b] $g_{av} = {}^1/_3(g_{xx} + g_{yy} + g_{zz} = {}^1/_3(2g_\perp + g_\parallel)$. [c] Aqueous spectra obtained at $T = 25.0$ °C. [d] Reference 3.

Table III. Dependence of the Absorbance (500 nm) of Nickel(III)–Triglycine Complexes on the Concentration of Triglycine[a]

$10^3[G_3]_T$, M	A	$10^3[G_3]_T$, M	A
0.06	0.038	37.48	0.064
6.32	0.050	49.98	0.066
18.80	0.057	80.0	0.078
31.28	0.061		

[a] $[Ni]_T = 5.6 \times 10^{-4}$ M; $[PO_4^{3-}]_T = 5.0 \times 10^{-2}$ M; $-\log [H^+] = 6.00$; $\mu = 0.1$; path length = 1.0 cm; $A_0 = 0.038$; $A_\infty = 0.078$; $pK_a[HG_3^*] = 7.88$[16].

pH values higher than 6.0 gave either complete formation of $Ni^{III}(H_{-2}G_3)(H_{-1}G_3)^{2-}$ or caused interference due to the base-catalyzed decomposition of $Ni^{III}(H_{-2}G_3)$.

The pK_{a2} of $Ni^{III}(H_{-2}G_3)_2^{3-}$, eq 3, was determined by means of a room-temperature titration with NaOH using EPR as a detector, Figure 3. The pK_{a2} value is 11.0 ± 0.1. This same value

$$Ni^{III}(H_{-2}G_3)(H_{-1}G_3)^{2-} \overset{K_{a2}}{\rightleftharpoons} Ni^{III}(H_{-2}G_3)_2^{3-} + H^+ \quad (3)$$

was obtained by monitoring the absorbance (307 nm) as a function of OH^-. The EPR method is useful for systems where the UV–visible spectra of the reactants and products of the titration are similar, as is the case here.

The corresponding five-nitrogen and six-nitrogen bis complexes of nickel(II) are not stable, and their stability constants are not known. However, it is instructive to compare the equilibrium constants for the mono(triglycine) complexes of nickel(II) with those of the bis complexes of nickel(III).

$$Ni^{2+} + G_3^- \overset{\beta_{1-11}}{\rightleftharpoons} Ni^{II}(H_{-1}G_3) + H^+ \quad (4)$$

$$Ni^{II}(H_{-1}G_3) \overset{K_{a2}}{\rightleftharpoons} Ni^{II}(H_{-2}G_3)^- + H^+ \quad (5)$$

The β_{1-11} value[16] is 7.9×10^{-6} for Ni(II), whereas the value for K_2 in eq 1 is 3.7×10^{-3}. Although the Ni(III) reaction is for the addition of a second G_3^- with less favorable electrostatics, and despite the need for the second G_3^- to replace a carboxylate group in order to give an N-coordinated peptide, K_2 is nevertheless $10^{2.7}$ times greater than β_{1-11}. This is attributed to the strength of the equatorial Ni(III)–N(peptide) bond. On the other hand, a comparison of the pK_a values of 11.0 in eq 3 with the value of 7.7 in eq 5 shows that the Ni(III) reaction is now $10^{3.3}$ times less favorable than the Ni(II) reaction. This reversal is consistent with the proposed structure of $Ni^{III}(H_{-2}G_3)_2^{3-}$, where an axially elongated peptide nitrogen forms a much weaker bond to Ni(III) than does the equatorial peptide nitrogen, and hence the deprotonation is more difficult.

Bis complexes of several other tripeptides were examined by EPR to determine the effect of the size of each amino acid residue on the formation of bis complexes. The following peptides form both the $Ni^{III}(H_{-2}L)(H_{-1}L)^{2-}$ and $Ni^{III}(H_{-2}L)_2^{3-}$ complexes: G_3, GAG, AGG, GleuG, AAG, GGA. Four tripeptides form only the $Ni^{III}(H_{-2}L)(H_{-1}L)^{2-}$ complex in appreciable quantity. They are A_3, GGleu, AGA, and GGF. Peptides that contain Aib in the third residue, G_2Aib, $AAib_2$, and Aib_3, do not form a bis complex. These results also support the proposed structures I and II. A tris complex with two peptides coordinated axially through their terminal amine nitrogens should not show such a steric effect

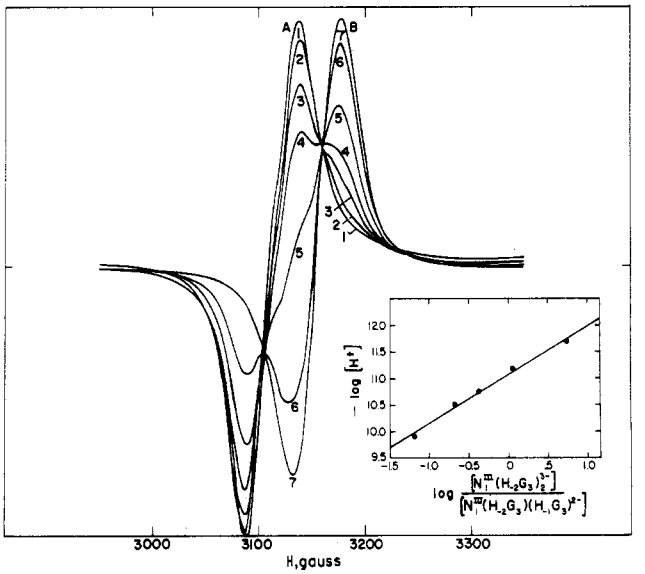

Figure 3. Aqueous EPR spectra at 22 °C of (A) 1.0×10^{-3} M $Ni^{III}(H_{-2}G_3)(H_{-1}G_3)^{2-}$ and (B) 1.0×10^{-3} M $Ni^{III}(H_{-2}G_3)_2^{3-}$ as a function of $-\log [H^+]$: (1) 9.06; (2) 9.89; (3) 10.52; (4) 10.78; (5) 11.17; (6) 11.67; (7) 12.18. Inset: plot used to calculate pK_{a2} (y intercept) from EPR spectral data.

whereas CPK models of the proposed bis species indicate that the size of the first and third peptide residue is critical to formation of the bis complexes.

Formation Kinetics. The kinetics of the formation of $Ni^{III}(H_{-2}L)(H_{-1}L)^{2-}$ were studied for a number of peptides (Table IV). A mechanism that is consistent with the data (L ≠ AGA or GGA) is proposed, eq 6–9, where $[Ni^{III}]_R = [Ni^{III}(H_{-2}L)] + [Ni^{III}(H_{-2}L)L^-]$. The preequilibrium step is proposed to explain a 0.1 absorbance unit jump (45% of the total absorbance change), which takes place during mixing on the stopped-flow apparatus. It also is consistent with the nonlinear dependence of k_{obsd} on ligand concentration. Resolved rate and equilibrium constants are given in Table V.

$$Ni^{III}(H_{-2}L) + L^- \overset{K_1}{\rightleftharpoons} Ni^{III}(H_{-2}L)L^- \quad (6)$$

$$Ni^{III}(H_{-2}L)L^- + OH^- \xrightarrow{k_1} Ni^{III}(H_{-2}L)(H_{-1}L)^{2-} + H_2O \quad (7)$$

$$\text{rate} = k_{obsd}[Ni^{III}]_R \quad (8)$$

$$k_{obsd} = \frac{k_1K_1[L^-][OH^-]}{1 + K_1[L^-]} \quad (9)$$

Combination of the K_1 value of 433 M^{-1} for G_3^- with its K_2 value of 3.7×10^{-3} permits a pK_{a1} value of 5.1 to be calculated for eq 10. Hence, the deprotonation step for this equatorial-N

$$Ni^{III}(H_{-2}G_3)G_3^- \overset{K_{a1}}{\rightleftharpoons} Ni^{III}(H_{-2}G_3)(H_{-1}G_3)^{2-} + H^+ \quad (10)$$

peptide is 6 orders of magnitude more favorable than for the subsequent axial-N peptide ($pK_{a2} = 11.0$).

A pH 6.4, where the formation reaction with G_3 was monitored, the concentration of hydroxide ion is small and the reaction is

Table IV. Observed First-Order Rate Constants for the Formation of $Ni^{III}(H_{-2}L)(H_{-1}L)^{2-}$ [a]

L	$10^3[L]_T$, M	$-\log [H^+]$	$10^3[HB]$, M	buffer	10^3k_{obsd}, s^{-1}
G_3	10.6	6.4	25.0	H_3PO_4	70 (1)
	12.5		7.0		59 (1)
	12.5		17.0		62 (2)
	12.5		42.0		68 (3)
	12.5		52.0		71 (2)
	21.1		25.0		124 (1)
	31.7		25.0		167 (4)
	42.3		25.0		199 (6)
	52.8		25.0		234 (4)
	155.0		25.0		375 (8)
AGG	13.7	7.0	25.0	H_3PO_4	98 (2)
	27.1				180 (2)
	40.7				248 (1)
	54.4				326 (1)
	67.8				419 (3)
GAG	30.0	8.0	25.0	H_3BO_3	88 (4)
	40.0				101 (3)
	50.0				113 (1)
GGA	40.0	8.0	25.0	H_3BO_3	152 (2)
	50.0				156 (9)
AGA	47.0	8.0	25.0	H_3BO_3	44 (5)
	70.5				40 (7)

[a] $[Ni^{III}(H_{-2}L)] = (5.0\text{–}5.4) \times 10^{-4}$ M; $\mu = 0.2$; $T = 25.0 \pm 0.2$ °C; $\lambda = 500$ nm.

partially carried by the phosphate buffer, HPO_4^{2-} (B^-), eq 11 and 12. The measurement of k_{obsd} with variation of the phosphate

$$Ni^{III}(H_{-2}G_3)G_3^- + B^- \overset{k_B}{\rightleftharpoons} Ni^{III}(H_{-2}G_3)(H_{-1}G_3)^{2-} + HB \quad (11)$$

$$k_{obsd} = (k_1[OH^-] + k_B[B^-])\frac{K_1[G_3^-]}{1 + K_1[G_3^-]} \quad (12)$$

buffer concentration (Table IV) permitted the resolution of rate constants: $k_B = 2.22$ M^{-1} s^{-1} and $k_1 = 8.9 \times 10^6$ M^{-1} s^{-1}. The concentration of buffer did not affect the observed rate constants of the reactions run at higher pH.

The magnitude of the equilibrium constants for coordination of NH_3 to various $Ni^{III}(H_{-2}L)$ complexes[25] is about 10^2. Ammonia ($pK_a = 9.29$) is a better nucleophile than a peptide amine ($pK_a = 7.88$[16] for triglycine). Therefore, the equilibrium constants presented in Table V for formation of $Ni^{III}(H_{-2}L)L^-$ are too large to be due to the second peptide acting as a monodentate ligand. Instead, a chelated species is proposed where a peptide oxygen of the second peptide displaces the carboxylate of the first peptide. The hydroxide-catalyzed step, eq 7, is then the exchange of a peptide nitrogen for the peptide oxygen. CPK models show that a methyl group on the middle peptide residue would sterically hinder this exchange, which explains why k_1 is 2 orders of magnitude smaller for GAG than for the other peptides.

The formation kinetics of $Ni^{III}(H_{-2}L)(H_{-1}L)^{2-}$ for L = AGA and GGA were also studied but were not clean first-order reactions. Base-catalyzed decomposition of $Ni^{III}(H_{-2}L)$ takes place at a rate similar to that of the formation of the bis species. A pH value could not be found where the formation of the bis complex was measureable and much faster than decomposition of $Ni^{III}(H_{-2}L)$. However, the data indicate that the formation rate is independent of ligand concentration. This implies that the rate-determining reaction has shifted to a step before that given in eq 6. It is proposed that the rate-determining step is now the opening of the carboxylate ring of $Ni^{III}(H_{-2}L)$. This is followed by rapid addition of the second peptide. The rate constant for the carboxylate ring opening for GGA and AGA is estimated from Table IV to be 0.10 ± 0.05 s^{-1}. The methyl group in the carboxylate peptide residue of GGA and AGA may be responsible for the decrease in the rate of the carboxylate ring-opening step.

(25) Murray, C. K.; Margerum, D. W. *Inorg. Chem.* **1982**, *21*, 3501–3506.

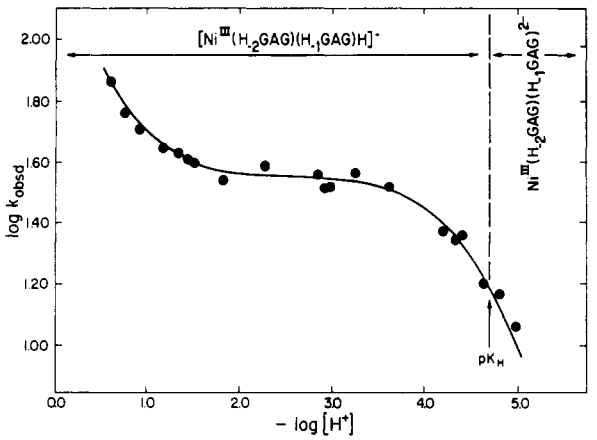

Figure 4. Dependence of the dissociation rate constant of $Ni^{III}(H_{-2}GAG)(H_{-1}GAG)^{2-}$ on acidity. The equilibrium and rate constants used to calculate the solid line are summarized in Table V.

A much higher concentration of hydroxide ion is needed to cause deprotonation of the second peptide nitrogen, eq 13, and this takes

$$Ni^{III}(H_{-2}G_3)(H_{-1}G_3)^{2-} + OH^- \xrightarrow{k_2} Ni^{III}(H_{-2}G_3)_2^{3-} + H_2O \quad (13)$$

place during the mixing process (4 ms) in the stopped-flow experiment. The value of k_2 is estimated to be greater than 1×10^5 M^{-1} s^{-1} by the assumption that at least 7 half-lives of the reaction take place during mixing at pH 12.

Acid-Catalyzed Dissociation Kinetics. When acid is added to a solution containing $Ni^{III}(H_{-2}GAG)_2^{3-}$ three reactions occur, eq 14–16. The first reaction is rapid and takes place during the

$$Ni^{III}(H_{-2}GAG)_2^{3-} + H^+ \rightarrow Ni^{III}(H_{-2}GAG)(H_{-1}GAG)^{2-} \quad (14)$$

$$Ni^{III}(H_{-2}GAG)(H_{-1}GAG)^{2-} + H^+ \rightarrow Ni^{III}(H_{-2}GAG) + GAG^- \quad (15)$$

$$Ni^{III}(H_{-2}GAG) + H^+ \rightarrow Ni^{II} \text{ products} \quad (16)$$

mixing time on the stopped-flow spectrophotometer. The second reaction, the dissociation of $Ni^{III}(H_{-2}GAG)(H_{-1}GAG)^{2-}$ to form the mono complex, has a complex hydrogen ion dependence as seen in Figure 4. The third reaction, redox decomposition of $Ni^{III}(H_{-2}GAG)$, is quite slow compared to the other reactions[26] and allows the kinetics of the acid dissociation reaction to be studied in detail (Table VI). A mechanism consistent with these data is proposed in eq 17–21 where $[Ni^{III}]_R = [Ni^{III}(H_{-2}GAG)(H_{-1}GAG)^{2-} + Ni^{III}(H_{-2}GAG)(H_{-1}GAG)H]^- + [Ni^{III}(H_{-2}GAG)(H_{-1}GAG)H^-]$. The mechanism is shown schematically in Scheme I.

$$Ni^{III}(H_{-2}GAG)(H_{-1}GAG)^{2-} + H^+ \overset{K_H}{\rightleftharpoons} [Ni^{III}(H_{-2}GAG)(H_{-1}GAG)H]^- \quad (17)$$

$$[Ni^{III}(H_{-2}GAG)(H_{-1}GAG)H]^- \xrightarrow{k_3} Ni^{III}(H_{-2}GAG) + GAG^- \quad (18)$$

$$[Ni^{III}(H_{-2}GAG)(H_{-1}GAG)H]^- + H^+ \xrightarrow{k_4} Ni^{III}(H_{-2}GAG) + H(GAG)^{\pm} \quad (19)$$

$$\text{rate} = k_{obsd}[Ni^{III}]_R \quad (20)$$

$$k_{obsd} = \frac{(k_3 + k_4[H^+])K_H[H^+]}{1 + K_H[H^+]} \quad (21)$$

Below pH 1.5, $K_H[H^+]$ is much greater than 1. Thus, eq 21 simplifies to eq 22. A plot of k_{obsd} vs. $[H^+]$ in this pH region

$$k_{obsd} = k_3 + k_4[H^+] \quad (22)$$

yields $k_3 = 34 \pm 1$ s^{-1} and $k_4 = 140 \pm 12$ M^{-1} s^{-1}. Rearrangement

(26) Loyola, V. M.; Subak, E. J., Jr.; Margerum, D. W., to be submitted for publication.

Table V. Equilibrium and Rate Constants for Bis(tripeptido)nickelate(III) Reactions (25.0 °C)

Equilibrium Constants	
Formation Reactions	
$Ni^{III}(H_{-2}G_3) + G_3^- \rightleftharpoons Ni^{III}(H_{-2}G_3)G_3^-$	$K_1 = 433 \pm 12\ M^{-1}$
$Ni^{III}(H_{-2}AGG) + AGG^- \rightleftharpoons Ni^{III}(H_{-2}AGG)AGG^-$	$K_1 = 27 \pm 7\ M^{-1}$
$Ni^{III}(H_{-2}GAG) + GAG^- \rightleftharpoons Ni^{III}(H_{-2}GAG)GAG^-$	$K_1 = 158 \pm 23\ M^{-1}$
$Ni^{III}(H_{-2}G_3) + G_3^- \rightleftharpoons Ni^{III}(H_{-2}G_3)(H_{-1}G_3)^{2-} + H^+$	$K_2 = (3.7 \pm 0.2) \times 10^{-3}$
Protonation and Deprotonation Equilibria	
$Ni^{III}(H_{-2}G_3)G_3^- \rightleftharpoons Ni^{III}(H_{-2}G_3)(H_{-1}G_3)^{2-} + H^+$	$\log K_{a1} = -5.1 \pm 0.1$
$Ni^{III}(H_{-2}G_3)(H_{-1}G_3)^{2-} \rightleftharpoons Ni^{III}(H_{-2}G_3)_2^{3-} + H^+$	$\log K_{a2} = -11.0 \pm 0.1$
$Ni^{III}(H_{-2}GAG)(H_{-1}GAG)^{2-} + H^+ \rightleftharpoons [Ni^{III}(H_{-2}GAG)(H_{-1}GAG)H]^-$	$\log K_H = 4.7 \pm 0.1$
Rate Constants	
Formation and Dissociation Reactions	
$Ni^{III}(H_{-2}G_3)G_3^- + OH^- \rightarrow Ni^{III}(H_{-2}G_3)(H_{-1}G_3)^{2-} + H_2O$	$k_1 = (8.9 \pm 0.2) \times 10^6\ M^{-1}\ s^{-1}$
$Ni^{III}(H_{-2}AGG)AGG^- + OH^- \rightarrow Ni^{III}(H_{-2}AGG)(H_{-1}AGG)^{2-} + H_2O$	$k_1 = (1.5 \pm 0.4) \times 10^7\ M^{-1}\ s^{-1}$
$Ni^{III}(H_{-2}GAG)GAG^- + OH^- \rightarrow Ni^{III}(H_{-2}GAG)(H_{-1}GAG)^{2-} + H_2O$	$k_1 = (1.3 \pm 0.1) \times 10^5\ M^{-1}\ s^{-1}$
$Ni^{III}(H_{-2}G_3)(H_{-1}G_3)^{2-} + OH^- \rightarrow Ni^{III}(H_{-2}G_3)_2^{3-} + H_2O$	$k_2 > 3 \times 10^4\ M^{-1}\ s^{-1}$
$[Ni^{III}(H_{-2}GAG)(H_{-1}GAG)H]^- \rightarrow Ni^{III}(H_{-2}GAG) + GAG^-$	$k_3 = 34 \pm 1\ s^{-1}$
$[Ni^{III}(H_{-2}GAG)(H_{-1}GAG)H]^- + H^+ \rightarrow Ni^{III}(H_{-2}GAG) + H(GAG)^*$	$k_4 = 140 \pm 12\ M^{-1}\ s^{-1}$
$Ni^{III}(H_{-2}G_3)G_3^- + HPO_4^{2-} \rightarrow Ni^{III}(H_{-2}G_3)(H_{-1}G_3)^{2-} + H_2PO_4^-$	$k_B = 2.22 \pm 0.05\ M^{-1}\ s^{-1}$

Table VI. Observed First-Order Rate Constants for the Reaction of $Ni^{III}(H_{-2}GAG)(H_{-1}GAG)^{2-}$ with Acid[a]

$-\log [H^+]$	$[HB]_T$, M	buffer	k_{obsd}, s^{-1}
0.60	0.250	$HClO_4$	71 (2)
0.76	0.175		56 (2)
0.90	0.125		50 (2)
1.10	0.080		42.2 (0.1)
1.32	0.025	$CHCl_2COOH$	44 (4)
1.44	0.025		40 (2)
1.50	0.025		38.0 (2)
1.83	0.025		31.6 (1.6)
2.84	0.015	$CH_2ClCOOH$	35.5 (0.7)
2.92	0.010		30.9 (1.3)
3.26	0.025		36 (3)
2.26	0.025	H_3PO_4	37.6 (1.6)
2.98	0.025		32.5 (1.2)
3.69	0.025		33 (3)
4.19	0.020	CH_3COOH	23.3 (0.1)
4.33	0.020		22.0 (0.5)
4.39	0.030		22.6 (0.5)
4.42	0.010		23.2 (0.3)
4.43	0.040		22.9 (0.9)
4.67	0.020		15.6 (0.8)
4.82	0.020		16.0 (0.3)
4.99	0.020		11.6 (0.2)

[a] $[Ni^{III}(H_{-2}GAG)(H_{-1}GAG)^{2-}]_0 = 2.5 \times 10^{-4}$ M; $\mu = 0.5$; $T = 25.0 \pm 0.2$ °C; $\lambda = 380$ nm.

of eq 21 yields a relationship suitable for determination of K_H, eq 23. From a plot of the left side of this equation vs. $1/[H^+]$,

$$\frac{k_3 + k_4[H^+]}{k_{obsd}} = \frac{1}{K_H[H^+]} + 1 \qquad (23)$$

the value of K_H is $(5.3 \pm 0.2) \times 10^4\ M^{-1}$.

The protonation constant, K_H, is proposed to be for an outside protonation (where the carboxylate group is protonated and hydrogen bonded to the peptide oxygen) rather than for the protonation of the peptide nitrogen. Similar protonations have been proposed for other oligopeptide complexes of Ni(II),[27] Cu(II),[28] Cu(III),[29] and Co(III).[30,31] Co(III) is much slower to substitute than the other metal ions, which allowed Freeman and coworkers[31] to isolate an outside-protonated bis(diglycinato)cobaltate(III) complex as a solid and to obtain a crystal structure, which indicated that the peptide oxygen was protonated.

Table VII. Redox Decomposition Products of Triglycine-Containing Nickel(III)–Peptide Complexes

peptide complex	pH	product	% original G_3 recovered as product
$Ni^{III}(H_{-2}G_3)_2^{3-}$[a]	13	G_3	36
		G_2a	8
		G_2	47
		2,5-piperazinedione	3
$Ni^{III}(H_{-2}G_3)(H_{-1}G_3)^{2-}$[b]	9	G_3	45
		G_2a	9
		G_2	41
		2,5-piperazinedione	2
$Ni^{III}(H_{-2}G_3)$[c]	9	G_3	56
		G_2a	7
		G_2	34
		2,5-piperazinedione	3

[a] $[Ni]_T = 9 \times 10^{-4}$ M; $[G_3]_0 = 3.6 \times 10^{-3}$ M. [b] $[Ni]_T = 8 \times 10^{-4}$ M; $[G_3]_0 = 3.2 \times 10^{-3}$ M; $[borate]_T = 2.0 \times 10^{-2}$ M. [c] $[Ni]_T = 8 \times 10^{-4}$ M; $[G_3]_0 = 8.8 \times 10^{-4}$ M; $[borate]_T = 2.0 \times 10^{-2}$ M.

The K_H determined in the present work is 2 orders of magnitude larger than the protonation constants reported for outside protonation of peptide oxygens.[27,28] However, it is of the same magnitude as the protonation constant reported for $Cu^{III}(H_{-3}G_4)^-$ ($K_H = 2.0 \times 10^4$).[29] In the G_4 case, the free carboxylate group is protonated and is proposed to be hydrogen bonded to the peptide oxygen. This same type of protonation is proposed for $[Ni^{III}(H_{-2}GAG)(H_{-1}GAG)H]^-$, structure III.

Base-Catalyzed Redox Decomposition. When solutions of bis(triglycinato)nickelate(III) complexes are made basic, a decoloration occurs in which the nickel(III) slowly oxidizes the peptide. The products of the reaction were determined by HPLC and compared to the products obtained from the base-catalyzed decomposition of $Ni^{III}(H_{-2}G_3)$. As can be seen in Table VII, the nature and the amount of the products are similar for the decomposition of $Ni^{III}(H_{-2}G_3)_2^{3-}$, $Ni^{III}(H_{-2}G_3)(H_{-1}G_3)^{2-}$, and $Ni^{III}(H_{-2}G_3)$. The main site of peptide oxidation is the carboxylate terminal peptide residue. A reaction sequence consistent with the product analysis is given in eq 24–27. The amount of initial G_3

$$2Ni^{III}(G_3)_n \rightarrow G_2aCH_2OH + CO_2 + Ni^{2+} + Ni^{II}(H_{-2}G_3)^- \qquad (24)$$

$$G_2aCH_2OH \rightarrow G_2a + HCHO \qquad (25)$$

$$G_2a + H_2O \rightarrow G_2^- + NH_3 \qquad (26)$$

$$G_2a \rightarrow 2,5\text{-piperazinedione} + NH_3 \qquad (27)$$

(27) Paniago, E. B.; Margerum, D. W. *J. Am. Chem. Soc.* **1972**, *94*, 6704–6710.
(28) Wong, L. F.; Cooper, J. C.; Margerum, D. W. *J. Am. Chem. Soc.* **1976**, *98*, 7268–7274.
(29) Rybka, J. S.; Kurtz, J. L.; Neubecker, T. A.; Margerum, D. W. *Inorg. Chem.* **1980**, *19*, 2791–2796.
(30) Hawkins, C. J.; Kelso, M. T. *Inorg. Chem.* **1982**, *21*, 3681–3686.
(31) Barnet, M. T.; Freeman, H. C.; Buckingham, D. A.; Hsu, I.; van der Helm, D. *J. Chem. Soc., Chem. Commun.* **1970**, 367–368.

Table VIII. Observed First-Order Rate Constants for the Redox Decomposition of Bis(triglycinato)nickelate(III) in Base[a]

$-\log [H^+]$	buffer	$10^3[\text{buffer}]_T$, M	$10^5 k_{obsd}$, s^{-1}
9.5	H_3BO_3	20	5.38
10.0	H_3BO_3	20	5.30
11.0	$NaHCO_3$	20	6.08
12.5	NaOH	32	8.14
12.6	H_3PO_4	20	8.30
13.0	NaOH	100	10.1

[a] $[Ni]_T = 1 \times 10^{-3}$ M; $T = 25.0 \pm 0.2$ °C; $\mu = 0.1$; $\lambda = 320$ nm.

recovered as product (G_3, G_2a, G_2, and 2,5-piperazinedione) equals 94–100%. However, an additional species with a retention time between that of G_3 and G_2a was observed. It corresponds to approximately 3% of the amount of G_3 originally present in solution. This species is believed to be diglycyl-*N*-(hydroxymethyl)amide, G_2aCH_2OH, because a similar species, G_3aCH_2OH (which eluted between G_4 and G_3a), was identified[12] as a product of the decomposition of $Ni^{III}(H_{-3}G_4)^-$. Production of G_2a and HCHO is consistent with hydrolysis of G_2aCH_2OH. Formaldehyde is a product of the decomposition reaction of the triglycine complexes of nickel(III) but is too poorly separated from the solvent front of the chromatogram to be quantitated.

The self-condensation product, 2,5-piperazinedione, has not been reported previously among the redox products of Ni(III)[12] or Cu(III)[29] tetrapeptide complexes. This may be due to differences in the time allowed between addition of base to the Cu(III) or Ni(III) solutions and product analysis. The nickel(III)–triglycine reactions were allowed to proceed for 24 h due to the slow decomposition of the bis complexes. During this period, G_2a slowly self-condenses to form 2,5-piperazinedione.

Alkaline solutions of $Ni^{III}(H_{-2}G_3)$ decompose much faster than alkaline solutions of $Ni^{III}(H_{-2}G_3)(H_{-1}G_3)^{2-}$ or $Ni^{III}(H_{-2}G_3)_2^{3-}$. The kinetics of the redox decomposition of the bis complexes were investigated as a function of pH (Table VIII). These rates can be compared to those of the base decomposition of mono complexes.[32] At pH 12.6, $Ni^{III}(H_{-2}GGA)$ decomposes 10^6 times faster than $Ni^{III}(H_{-2}G_3)_2^{3-}$, and at pH 9.0, $Ni^{III}(H_{-2}GGA)$ decomposes 10^3 times faster than $Ni^{III}(H_{-2}G_3)(H_{-1}G_3)^{2-}$. In other studies[33] it has been observed that the rates of decomposition of copper(III) peptides increase greatly as their electrode potentials increase. The large differences in rate for the nickel(III) complexes may also be due to differences in the reduction potentials of the complexes where the $E°'$ values are $Ni^{III}(H_{-2}L) > Ni^{III}(H_{-2}L)(H_{-1}L)^{2-} > Ni^{III}(H_{-2}G_3)_2^{3-}$. This order agrees with the number of strong electron-donating groups coordinated to the metal.

A mechanism consistent with the data in Table VIII is proposed in eq 28–34, where $K_{OH} = K_{a2}/K_w$. The data are plotted in Figure

$$Ni^{III}(H_{-2}G_3)(H_{-1}G_3)^{2-} + OH^- \overset{K_{OH}}{\rightleftharpoons} Ni^{III}(H_{-2}G_3)_2^{3-} \quad (28)$$

$$Ni^{III}(H_{-2}G_3)(H_{-1}G_3)^{2-} \xrightarrow{k_5} Ni^{II} \text{ products} \quad (29)$$

$$Ni^{III}(H_{-2}G_3)(H_{-1}G_3)^{2-} + OH^- \xrightarrow{k_6} Ni^{II} \text{ products} \quad (30)$$

$$Ni^{III}(H_{-2}G_3)_2^{3-} \xrightarrow{k_7} Ni^{II} \text{ products} \quad (31)$$

$$Ni^{III}(H_{-2}G_3)_2^{3-} + OH^- \xrightarrow{k_8} Ni^{II} \text{ products} \quad (32)$$

$$\text{rate} = k_{obsd}[Ni^{III}]_T \quad (33)$$

$$k_{obsd} = \frac{k_5 + k_6[OH^-] + k_7K_{OH}[OH^-] + k_8K_{OH}[OH^-]^2}{1 + K_{OH}[OH^-]} \quad (34)$$

5 where the solid line is calculated from eq 34 by using $k_5 = 5.2 \times 10^{-5}$ s^{-1}, $(k_6 + k_7K_{OH}) = 7.2 \times 10^{-2}$ M^{-1} s^{-1}, and $k_8 = 3.0 \times 10^{-4}$ M^{-1} s^{-1}. The constants k_6 and k_7 cannot be resolved in this mechanism.

(32) Bowers, C. P.; Margerum, D. W., unpublished results.
(33) Nagy, J. C.; Diaddario, L. L.; Farkas, J. M.; Margerum, D. W., to be submitted for publication.

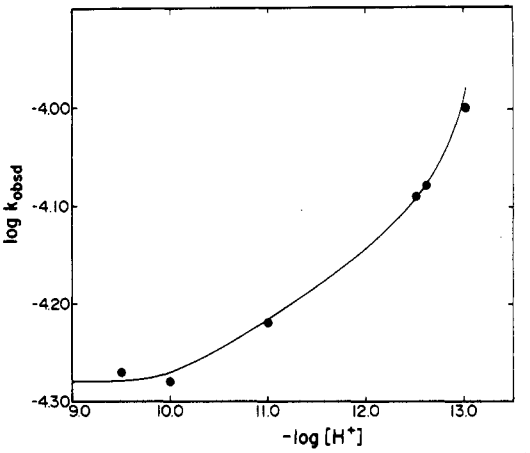

Figure 5. Dependence of the redox decomposition rate constant of bis(triglycinato)nickelate(III) on acidity. The solid line is calculated from eq 34.

Nickel(II) Peptides. The electrochemistry of the bis(tripeptido)nickelate(III/II) system is complicated due to chemical irreversibility. The $Ni^{II}(H_{-2}L)^-$ complex is much more stable than $Ni^{II}(H_{-2}L)_2^{4-}$ or $Ni^{II}(H_{-2}L)(H_{-1}L)^{3-}$. In fact, potentiometric titrations of solutions containing up to 0.105 M triglycine and 5.0×10^{-2} M nickel(II) fail to reveal any $Ni^{II}(H_{-2}L)_2^{4-}$ or $Ni^{II}(H_{-2}L)(H_{-1}L)^{3-}$. Instead, the major species are $Ni^{II}(H_{-2}G_3)^-$, $Ni^{II}(H_{-1}G_3)_2^{2-}$, and $Ni^{II}(H_{-1}G_3)(G_3)_2^{2-}$. The stability constants of the latter two species were determined by potentiometric titrations and are $\log \beta_{1-22} = -11.79$ (0.09) and $\log \beta_{1-13} = -0.247$ (0.087). These constants are in good agreement with those found previously from spectrophotometric data.[34]

There is evidence from redox reactions that $Ni^{II}(H_{-2}G_3)_2^{4-}$ and $Ni^{II}(H_{-2}G_3)(H_{-1}G_3)^{3-}$ can have a transitory existence. When a large concentration of ascorbate or hydroxylamine is mixed with $Ni^{III}(H_{-2}G_3)(H_{-1}G_3)^{2-}$, electron transfer occurs during the mixing process. Following electron transfer, another reaction is observed, which is proposed to be the loss of a peptide from the nickel(II) bis complex, eq 35. At pH 9.0 $k_{10} = 150$ s^{-1} and is independent

$$Ni^{II}(H_{-2}G_3)(H_{-1}G_3)^{3-} + H_2O \xrightarrow{k_{10}} Ni^{II}(H_{-2}G_3)^- + G_3^- + OH^- \quad (35)$$

of the concentration of reductant.

Reduction Potentials. In alkaline solutions, pH >10, the reduction potential of $Ni^{III/II}(H_{-2}L)^{0/-}$ is pH dependent, decreasing with increasing pH. This implies further deprotonation of the nickel(III) complex. There is no spectral evidence of amine-deprotonated nickel(III)–tripeptide complexes. Therefore, deprotonation of an axially coordinated H_2O molecule is proposed, eq 36. Values of pK_{a3} vary with tripeptide and are 10.4 and 11.2

$$Ni^{III}(H_{-2}L) \overset{K_{a3}}{\rightleftharpoons} Ni^{III}(H_{-2}L)OH^- + H^+ \quad (36)$$

for L = GAG and A_3, respectively.

The reduction potentials of the bis(tripeptide) complexes could not be determined accurately because of the instability of the corresponding nickel(II) complexes. Cyclic voltammograms of solutions of $Ni^{III}(H_{-2}G_3)(H_{-1}G_3)^{2-}$ show only a cathodic wave at scan rates less than 2 V/s. Attempts to scan faster than the dissociation rate of $Ni^{II}(H_{-2}G_3)(H_{-1}G_3)^{3-}$ were unsuccessful due to the sluggish heterogeneous kinetics that are typically encountered with all nickel(III)–peptide complexes.

Cyclic voltammograms of solutions of $Ni^{III}(H_{-2}G_3)_2^{3-}$ (at $[OH^-] = 0.1$ M) show an electrochemically reversible wave (peak separation of 60–70 mv) at $E_{1/2} = 0.66$ V (vs. NHE). However, the peak current is directly proportional to the scan rate, which indicates adsorption of the complex to the electrode. Adsorption takes place at pH values greater than 11.6 on all the electrodes

(34) Czarnecki, J. J. Ph.D. Thesis, Purdue University, 1976.

Scheme II

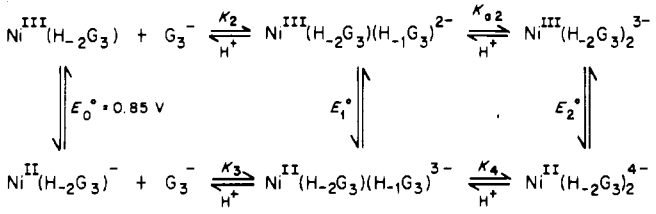

Table IX. Second-Order Rate Constants for the Reaction of $Fe^{II}(CN)_6^{4-}$ with Bis(triglycinato)nickelate(III)[a]

−log [H⁺]	$10^3[G_3^-]$, M	10^3k, M^{-1} s^{-1}	−log [H⁺]	$10^3[G_3^-]$, M	10^3k, M^{-1} s^{-1}
9.0	0.20	15.98 ± 0.01	10.5	0.20	13.1 ± 0.2
9.0	0.70	15.2 ± 0.6	11.0	0.20	9.13 ± 0.05
9.0	1.70	15.4 ± 0.3	11.5	0.20	5.10 ± 0.02
9.0	2.70	15.8 ± 0.3	12.0	0.20	1.79 ± 0.02
9.0	25.0	16.2 ± 0.2	13.0	0.20	0.438 ± 0.03
10.0	0.20	14.5 ± 0.1	13.7	0.20	0.380 ± 0.01

[a] $[Ni^{III}]_T = 5 \times 10^{-5}$ M; $\mu = 0.1$; $T = 25.0 \pm 0.2$ °C; $\lambda = 350$ nm.

at which the nickel(III) complexes are active: glassy carbon, graphite, and carbon paste.

Estimates of the reduction potentials of $Ni^{III/II}(H_{-2}G_3)(H_{-1}G_3)^{2-/3-}$ ($E_1°$) and $Ni^{III/II}(H_{-2}G_3)_2^{3-/4-}$ ($E_2°$) were calculated from the thermodynamic cycles presented in Scheme II. The equilibrium constants K_2 and K_{a2} are known from eq 1 and 3, respectively, and the value of $E_0°$ is known.[2] However, the equilibrium constants $K_3 = ([Ni^{II}(H_{-2}G_3)(H_{-1}G_3)^{3-}][H^+])/([Ni^{II}(H_{-2}G_3)^-][G_3^-])$ and $K_4 = ([Ni^{II}(H_{-2}G_3)_2^{4-}][H^+])/[Ni^{II}(H_{-2}G_3)(H_{-1}G_3)^{3-}]$ are not known. Our potentiometric titration results indicate that $Ni^{II}(H_{-2}G_3)_2^{4-}$ and $Ni^{II}(H_{-2}G_3)(H_{-1}G_3)^{3-}$ are not present in significant concentrations (<2% of Ni_T) at $[G_3^-] = 0.105$ M, pH 12. Therefore, K_3 must be less than 2×10^{-13} and K_4 must be less than 1×10^{-12}. From these estimates of K_3 and K_4, $E_1° < 0.24$ V and $E_2° < 0.19$ V (vs. NHE).

While these reduction potentials are only estimates, they are significantly lower than the 0.80–0.89-V (vs. NHE) reduction potentials of the mono(tripeptide) complexes.[2] Two phenomena are responsible for this difference. First, the bis(tripeptido)nickelate(III) complexes are more stable than the mono complexes due to coordination of additional deprotonated peptide nitrogens in the bis complexes. Secondly, the bis complexes of nickel(II) are much less stable than $Ni^{II}(H_{-2}L)^-$. Since the reduction potential is a measure of the energy difference between nickel(III) and nickel(II), either the destabilization of nickel(II) or the stabilization of nickel(III) will lower the reduction potential.

Electron Transfer. Cross-exchange electron-transfer reactions were used to determine whether the second peptide is removed prior to the reduction of nickel(III). Hexacyanoferrate(II) rate constants for the reduction of $Ni^{III}(H_{-2}G_3)_2^{3-}$ and $Ni^{III}(H_{-2}G_3)(H_{-1}G_3)^{2-}$ are given in Table IX. The reaction is pH dependent, and the solid line in Figure 6 is calculated from k_{obsd} based on the mechanism in eq 37–41, where $k_9 = 1.6 \times 10^4$ M^{-1} s^{-1} and $k_{10} = 380$ M^{-1} s^{-1}. The fit to this mechanism requires the electron transfer to take place prior to loss of the second peptide. Also, the rate constants are independent of the concentration of excess triglycine. If G_3^- were lost before the redox reaction, an inverse dependence on triglycine concentration would have been found.

$$Ni^{III}(H_{-2}G_3)(H_{-1}G_3)^{2-} \overset{K_{a2}}{\rightleftharpoons} Ni^{III}(H_{-2}G_3)_2^{3-} + H^+ \quad (37)$$

$$Ni^{III}(H_{-2}G_3)(H_{-1}G_3)^{2-} + Fe^{II}(CN)_6^{4-} \xrightarrow{k_9} Ni^{II} \text{ products} + Fe^{III}(CN)_6^{3-} \quad (38)$$

$$Ni^{III}(H_{-2}G_3)_2^{3-} + Fe^{II}(CN)_6^{4-} \xrightarrow{k_{10}} Ni^{II} \text{ products} + Fe^{III}(CN)_6^{3-} \quad (39)$$

$$\text{rate} = k_{obsd}[Ni^{III}]_T \quad (40)$$

$$k_{obsd} = \frac{k_9[H^+] + k_{10}K_{a2}}{K_{a2} + [H^+]}[Fe^{II}(CN)_6^{4-}] \quad (41)$$

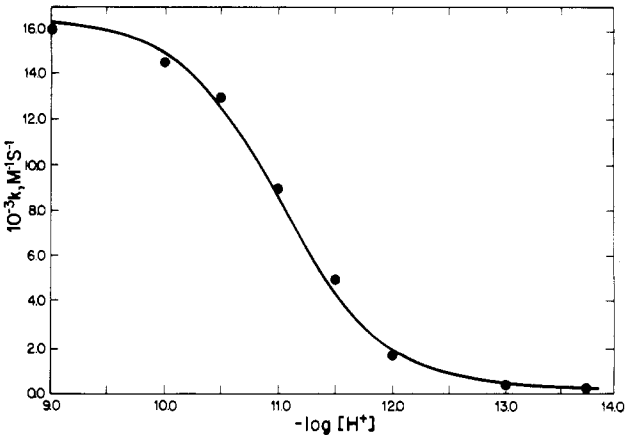

Figure 6. Dependence of the electron-transfer cross-exchange rate constant of the reaction of $Fe^{II}(CN)_6^{4-}$ with bis(triglycinato)nickelate(III) on acidity. The equilibrium and rate constants used to calculate the solid line are contained in Tables V and X, respectively.

Table X. Cross-Exchange Reactions of Nickel(III)–Tripeptide Complexes[a]

oxidant	reductant	$E°'_{red}$,[b] V	k_{12}, M^{-1} s^{-1}
$Ni^{III}(H_{-2}G_3)_2^{3-}$	$Fe^{II}(CN)_6^{4-}$	0.42	380
	$W^{IV}(CN)_8^{4-}$	0.54	147
	$Cu^{II}(H_{-3}Aib_3a)^-$	0.37	8.19
	$Cu^{II}(H_{-2}Aib_3)^-$	0.66	7.67×10^{-2}
$Ni^{III}(H_{-2}G_3)(H_{-1}G_3)^{2-}$	$Fe^{II}(CN)_6^{4-}$	0.42	16000
	$W^{IV}(CN)_8^{4-}$	0.54	3700
	$Cu^{II}(H_{-3}Aib_3a)^-$	0.37	244
	$Cu^{II}(H_{-2}Aib_3)^-$	0.66	0.417
	ascorbate	0.72[c]	4500
$Ni^{III}(H_{-2}A_3)$	$Fe^{II}(CN)_6^{4-}$	0.42	7×10^7[d]
	$W^{IV}(CN)_8^{4-}$	0.54	5×10^7[d]
	$Cu^{II}(H_{-2}Aib_3)^-$	0.66	1.8×10^5[e]

[a] $\mu = 0.1$; $T = 25.0 \times 0.2$ °C. [b] Measured vs. NHE. [c] Williams, N. H.; Yandell, J. K. *Aust. J. Chem.* **1982**, *35*, 1133–1134. [d] Reference 35. [e] Owens, G. D.; Phillips, D. A.; Czarnecki, J. J.; Raycheba, J. M. T.; Margerum, D. W. *Inorg. Chem.* **1984**, *23*, 1345–1353.

Several other electron-transfer reactions involving the bis complexes of nickel(III) were studied (Table X). Reductants include $W^{IV}(CN)_8^{4-}$, $Cu^{II}(H_{-3}Aib_3a)^-$, $Cu^{II}(H_{-2}Aib_3)^-$, and ascorbate. In all cases, the bis(tripeptido)nickelate(III) complexes react significantly slower than do the mono complexes. This can largely be attributed to the difference in the thermodynamic driving force of the reactions, because the reduction potentials of the bis complexes are much lower than those of the mono complexes. However, some of the difference may be due to the mechanism by which the electron transfers from the reductant to the nickel(III).

Electron-transfer between $Ni^{III}(H_{-2}L)$ and $Fe^{II}(CN)_6^{4-}$ or $W^{IV}(CN)_8^{4-}$ is thought to proceed via an inner-sphere mechanism caused by coordination of the reductant to the nickel(III) through a cyanide bridge.[35] This proposal is based on the observation that the experimentally determined cross-exchange rate constants, k_{12}, are 10^2–10^5 times larger than the rate constants predicted by Marcus'[36] theory for outer-sphere electron transfer.

Coordinatively saturated $Ni^{III}(H_{-2}L)_2^{3-}$ is unlikely to break a metal–peptide chelate bond in order to allow cyanide to bridge the reductant to the metal. Therefore, the electron-transfer reaction with $Fe(CN)_6^{4-}$ should follow an outer-sphere mechanism.

(35) Dennis, C. R.; Nemeth, M. T.; Kumar, K.; Margerum, D. W., to be submitted for publication.
(36) Marcus, R. A. *J. Phys. Chem.* **1963**, *67*, 853–857.

It is not clear, however, whether a peptide oxygen or a water molecule occupies the second axial site of $Ni^{III}(H_{-2}L)(H_{-1}L)^{2-}$. A bridging cyanide would probably not replace a peptide oxygen before electron transfer but might replace a water molecule, as is the case for the mono complexes. CPK models indicate that coordination of the peptide oxygen is possible. Furthermore, coordination of the peptide oxygen would provide an additional chelate ring and thus stabilize the $Ni^{III}(H_{-2}L)(H_{-1}L)^{2-}$ complex. The cross-exchange rate constants of $Ni^{III}(H_{-2}G_3)(H_{-1}G_3)^{2-}$ are only 5-42 times larger than those of $Ni^{III}(H_{-2}G_3)_2^{3-}$. This factor appears to be too small to be due to an inner-sphere pathway where factors of up to 10^5 were found. Therefore, the $Ni^{III}(H_{-2}G_3)(H_{-1}G_3)^{2-}$ electron-transfer reactions are proposed to be outer sphere and the peptide oxygen coordinated axially. However, this argument is based on the assumption that the reduction potential of $Ni^{III}(H_{-2}G_3)_2^{3-}$ is less than or equal to that of $Ni^{III}(H_{-2}G_3)(H_{-1}G_3)^{2-}$, which is likely but as yet not proven.

Conclusions

Bis(tripeptido)nickelate(III) complexes of non sterically hindered peptides can be expected to form in neutral or alkaline solution whenever there is excess tripeptide present. These complexes are less reactive than the mono complexes in both electron-transfer and redox decomposition reactions but react rapidly with acid to give the mono complexes. The reduction potentials of the bis complexes are significantly (at least 0.56 V) lower than those of the mono complexes.

Acknowledgment. This investigation was supported by Public Health Service Grant No. GM 12152 from the National Institute of General Medical Sciences and by a fellowship from Chevron Research (G.E.K.).

Registry No. $Ni^{III}(H_{-2}G_3)_2^{3-}$, 97764-72-2; $Ni^{III}(H_{-2}G_3)(H_{-1}G_3)^{2-}$, 97764-73-3; $Ni^{III}(H_{-2}G_3)$, 97764-74-4; $Ni^{II}(H_{-2}G_3)^-$, 97764-75-5; $Ni^{III}(H_{-2}AGG)(H_{-1}AGG)^{2-}$, 97764-76-6; $Ni^{III}(H_{-2}GAG)(H_{-1}GAG)^{2-}$, 97764-77-7; $Ni^{III}(H_{-2}GGA)(H_{-1}GGA)^{2-}$, 97764-78-8; $Ni^{III}(H_{-2}AGA)(H_{-1}AGA)^{2-}$, 97764-79-9; $Ni^{III}(H_{-2}AGG)$, 97764-80-2; $Ni^{III}(H_{-2}GAG)$, 97764-81-3; $Ni^{III}(H_{-2}GGA)$, 97764-82-4; $Ni^{III}(H_{-2}AGA)$, 97781-33-4; G_3, 556-33-2; G_2a, 20238-94-2; G_2, 556-50-3; $Ni^{III}(H_{-2}A_3)$, 97764-83-5; $Ni^{II}(H_{-2}G_3)(H_{-1}G_3)^{3-}$, 97764-84-6; $Ni^{II}(H_{-2}G_3)_2^{4-}$, 97764-85-7; $Fe^{II}(CN)_6^{4-}$, 13408-63-4; $W^{IV}(CN)_8^{4-}$, 18177-17-8; $Cu^{II}(H_{-3}Aib_3a)^-$, 85926-43-8; $Cu^{II}(H_{-2}Aib_3)^-$, 89438-84-6; 2,5-piperazinedione, 106-57-0; ascorbic acid, 50-81-7.

Contribution from the Department of Inorganic and Physical Chemistry, Indian Institute of Science, Bangalore 560 012, India

Electrochemical Redox Properties and Spectral Features of Supermolecular Porphyrins

G. BHASKAR MAIYA and V. KRISHNAN*

Received December 28, 1984

meso-(Tetrakis(benzo-15-crown-5)porphyrin (TCP) and its metal (Mg(II), $V^{IV}O$, Ni(II), Cu(II), Zn(II), and Mn(III)) derivatives form dimers on complexation with K^+ ions. The porphyrin ring oxidations of these dimers are found to occur at less anodic potentials relative to the oxidations of the corresponding monomers. The electrochemical redox states of these dimers in conjunction with their electronic absorption and emission features have been used to arrive at the electronic structures. Supermolecular formalism has been proposed to describe the properties of these dimers. EPR data on the oxidized dimer radical cations indicate that the unpaired electron is localized on one of the porphyrin π systems unlike those found in the reaction-center complex, "special pair" bacteriochlorophyll (BChl) molecules, of the bacterial photosynthetic system.

Introduction

Supermolecular systems constitute two identical molecular entities coexisting together without the assistance of a covalent linkage. The notable features of these systems are (i) they exhibit spectral features different from those of the individual molecular units and (ii) they display reactivity patterns incommensurate with those of the component molecular entities. Polynuclear aromatic hydrocarbons are well-known to form supermolecular systems.[1] In our earlier studies on tetrakis(5,10,15,20-benzo-15-crown-5)-porphyrin (TCP) and its metal derivatives (MTCP), we demonstrated[2] the formation of dimeric porphyrins when TCP or MTCP is complexed with cations, e.g. K^+, Ba^{2+}, and NH_4^+ (Figure 1). These molecules are described as supermolecules since the two porphyrin units are joined by noncovalent interactions and exhibit optical absorption and emission properties different from those of the monomeric porphyrin units. In the anticipation that these dimeric porphyrins should exhibit different redox properties relative to those of the monomeric units, we carried out electrochemical redox potential measurements on these dimers. It is known[3] that the potentials of reversible one-electron oxidations and reductions of conjugated aromatic systems provide a good experimental estimate of the relative energies of the highest occupied molecular orbital (HOMO) and the lowest unoccupied molecular orbital (LUMO), respectively. In view of the close analogy between the π systems of the conjugated aromatic hydrocarbons and porphyrins, the redox potentials of the latter should yield the energies of the HOMO and LUMO, which would be useful in the supermolecular description of the crown porphyrin dimers.

The objectives of this study are (i) to seek the manner in which the ring oxidation potentials (energies of the HOMO) of the dimers change with respect to corresponding monomeric species, (ii) to investigate the effect of the central metal ion on the redox properties of the dimers, and (iii) to study the influence of spatial constraint of the dimers on the electronic spectral features and the magnitudes of oxidation potentials. For this reason, we have chosen only those metallic crown porphyrins [M = Mg(II), V(IV), Ni(II), Cu(II), Zn(II), and Mn(III)] where the first oxidation potential corresponds to one-electron transfer from the porphyrin ring to the electrode. Moreover, the optical and magnetic resonance studies of the dimers carried out in the present study provide a basis for the supermolecular description of these dimeric crown porphyrins.

Experimental Section

TCP and its metal derivatives [$V^{IV}O$, Ni(II), Cu(II), and Zn(II)] were synthesized according to the methods described.[2] Mn(III) and Mg(II) derivatives were synthesized according to the published procedures.[4] Dimeric crown porphyrins were produced on addition of excess KCl (AR

(1) (a) Doris, K. A.; Ellis, D. E.; Ratner, M. A.; Marks, T. J. *J. Am. Chem. Soc.* **1984**, *106*, 2491-2497. (b) Meot-ner, M. *J. Phys. Chem.* **1980**, *84*, 2724-2729. (c) Kira, A.; Imamura, M.; Shida, T. *J. Phys. Chem.* **1976**, *80*, 1445-1451. (d) Howarth, O. W.; Fraenkel, G. K. *J. Am. Chem. Soc.* **1966**, *88*, 4514-4516.

(2) (a) Thanabal, V.; Krishnan, V. *J. Am. Chem. Soc.* **1982**, *104*, 3643-3650. (b) Thanabal, V.; Krishnan, V. *Inorg. Chem.* **1982**, *21*, 3606-3610.

(3) Felton, R. H. In "The Porphyrins"; Dolphin, D., Ed.; Academic Press: New York, 1978; Vol. 5, Part C, Chapter 3.

(4) Fuhrhop, J.-H.; Smith, K. M. In "Porphyrins and Metalloporphyrins"; Smith, K. M., Ed.; Elsevier: Amsterdam, 1975; Chapter 19, pp 757-869.

0020-1669/85/1324-3253$01.50/0